

Biomechanical Analysis of Rapid Maxillary Expansion in Adult Human Skull

Baldawa Rahul Shyamsunder*, Bhad Wasundhara Ashok**

Abstract

Objectives: To evaluate the biomechanical effects of rapid maxillary expansion (RME) on the craniofacial complex as applied to three-dimensional model of an adult human skull using the finite element method.

Materials & Methods: A 3-dimensional FEM of the craniofacial complex was developed from sequential computed tomography scan images by using the MIMICS software (version 8.0, Materialise, Leuven, Belgium) and ANSYS software (version 8.0). Known transversal (X) displacement with magnitudes of 1 mm, 3 mm and 5 mm were applied on the maxillary canine and first molar crown. The displacement and von-Mises stresses in different planes were studied on different nodes located at various structures of the craniofacial complex.

Results: Transverse orthopedic forces not only produced an expansive force at the intermaxillary suture but also high forces on various structures of the craniofacial complex, particularly at the base of the sphenoid bone and frontal process of the zygomatic bone. Lateral bending of the free ends of the pterygoid plates were noted, with increased resistance demonstrated in superior parts attached to the cranial base.

Conclusion: RME must be used judiciously in adults because of its far - reaching effects involving heavy stresses being noted at the sphenoid bone, zygomatic bone, nasal bone and their adjacent sutures.

Keywords: Adult; Biomechanical effect; Craniofacial complex; Finite element method; Rapid maxillary expansion.

Introduction

Interest in use of rapid maxillary expansion (RME) in adult patients has increased markedly during the past 2 decades. The correction of transverse discrepancies and the gain in arch perimeter as a potential non extraction technique appear to be the most important reasons underlying this increased interest.[1] Although the major treatment effect is noticed clinically in the area of the

dentition, transverse enlargement of the apical base or the skeletal structures throughout the nasomaxillary complex occur simultaneously.

The review by Bishara and Staley[2] and the orthodontic texts by Proffit[3] as well as by McNamara and Brudon[4], all state that the feasibility of palatal expansion beyond the late teens and early twenties is questionable.

In order to overcome the resistance of the adult sutures to expansion, "surgically assisted" rapid maxillary expansion (SA-RME) has been advocated. SA-RME procedures have traditionally been thought to have a low morbidity, but this surgery is not free of risks, and it behooves surgeons to be aware of its potential complications.

In view of the negative outlook for successful nonsurgical palatal expansion in adult patients and concerns about the potential complications and hazards of surgical procedure, it seemed appropriate to evaluate the biomechanical effects of

Authors affiliation: *Sr. Lecturer, Rural Dental College, Loni 413 736, Tal. Rahata, Dist. Ahmednagar, India, **Asso. Professor and Head, Dept. of Orthodontics and Dentofacial Orthopedics, Government Dental College and Hospital, Nagpur 440 003, India.

Reprints requests: Dr. Baldawa Rahul Shyamsunder, 302, Department of Orthodontics and Dentofacial Orthopedics, Rural Dental College, Loni 413 736, Tal. Rahata, Dist. Ahmednagar, Maharashtra, India.

E-mail: baldawars1@rediffmail.com

(Received on 10.12.2012, accepted on 22.03.2013)

nonsurgical RME in adults.

This paper aims at investigating the biomechanical effects of RME on the craniofacial complex as applied to a three-dimensional model of an adult human skull. Within this context, the objectives of this study are:

1. To construct an anatomically accurate three-dimensional finite element model of the craniofacial complex of an adult human.

2. To apply simulated displacement to the model, to know the structures involved and quantify the resultant stresses within the craniofacial complex, and to discuss the relationship of these stresses to the induced biological phenomenon.
3. To investigate the hypothesis that when RME is undertaken, the anatomical structures and the sutures of the nasomaxillary complex influence the force necessary and the manner in which the maxillae open.

Figure 1: Dried adult human skull used in this study



Material and Methods

The analytical model in this study was developed from a dry human skull of an adult female (Fig 1) with an approximate age of 20 years, selected from the anatomic collection.

Previous studies[5] have used photographs of cross-sections of skull. In the present study, CT scan images of the skull excluding the mandible were taken in the axial direction, parallel to the Frankfort horizontal plane. Sequential CT images were taken at 1mm intervals to reproduce finer and detailed aspects of the geometry (Fig 2). This spacing

Figure 2: Sample CT slices

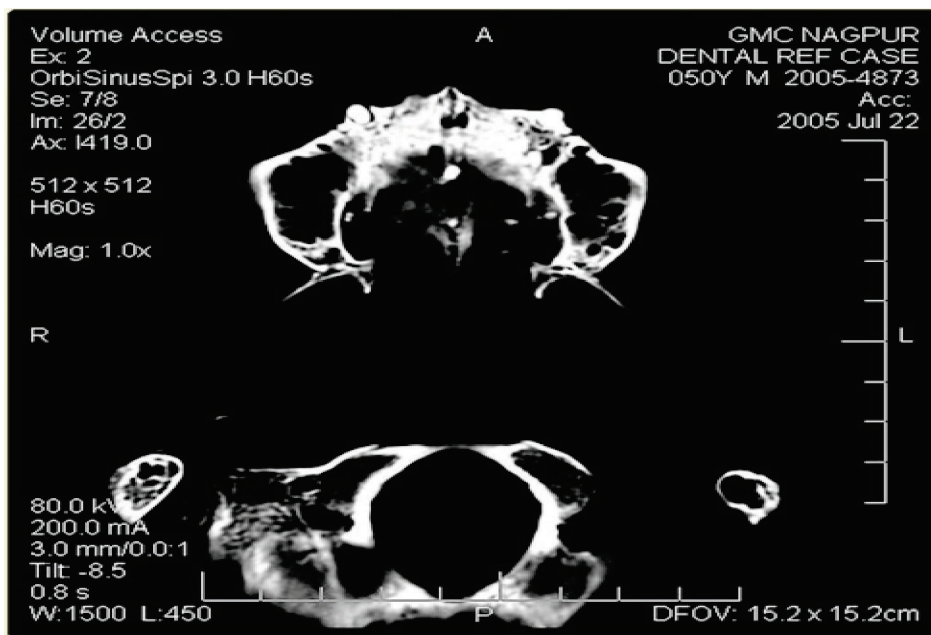
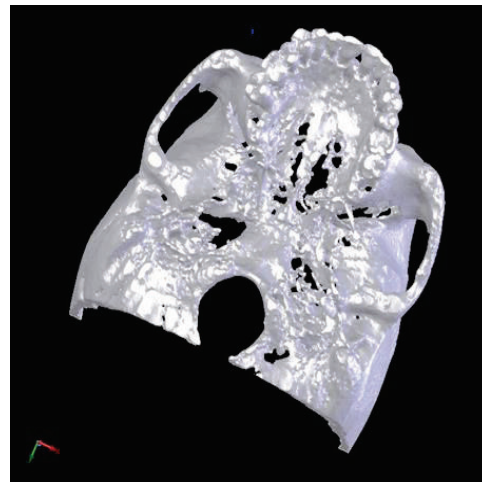
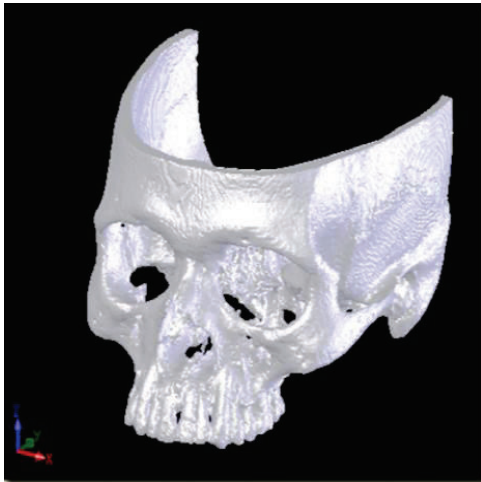


Figure 3 A, B: Different views of 3-D reconstruction of CT scans of skull



of CT-images enabled a higher geometric accuracy than that used by Jafari *et al* (2003; 5 mm)[6]; Iseri *et al* (1998; 5 mm)[7] and Tanne *et al* (1989; 10mm).[5]

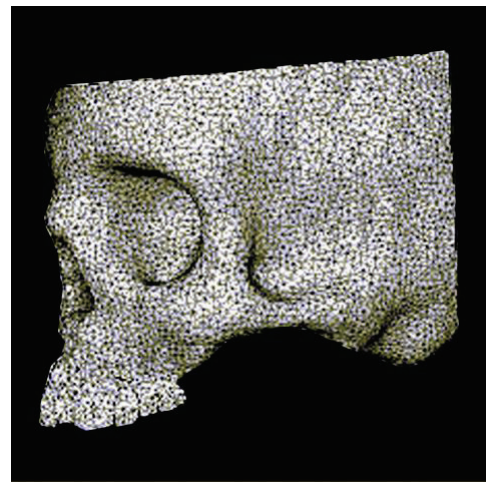
The CT scan images were read into visualization software – MIMICS. Materialise’s Interactive Medical Image Control System (MIMICS) is an interactive tool for the visualization and segmentation of CT images as well as MRI images and 3D rendering of objects (Fig 3A, B). In this model, Tet 10 solid elements (10 noded) were used. The model consisted of 7,13,009 nodes and 3,57,425 Tet 10 elements (Fig 4).

The materials in the analysis were assumed to be linearly elastic and isotropic. The mechanical properties of the compact and cancellous bones and teeth in the model were defined according to the experimental data in previous studies[5-7] as shown in Table I. All sutures were assumed to have the same mechanical properties as the surrounding bone material except at the palatal bone.

The two parts of the palatal bone that are separated by the vertical plane of symmetry were assumed to be unconnected, so that they moved freely in lateral directions with respect to the vertical plane of symmetry. This was done to investigate the stress distribution and deformation of the craniofacial complex after splitting of the midpalatal suture.

All other points of the cranium lying on the symmetry plane were constrained to have no

Figure 4: Lateral view of the final 3-D finite element model constructed using Tet 10 solid elements

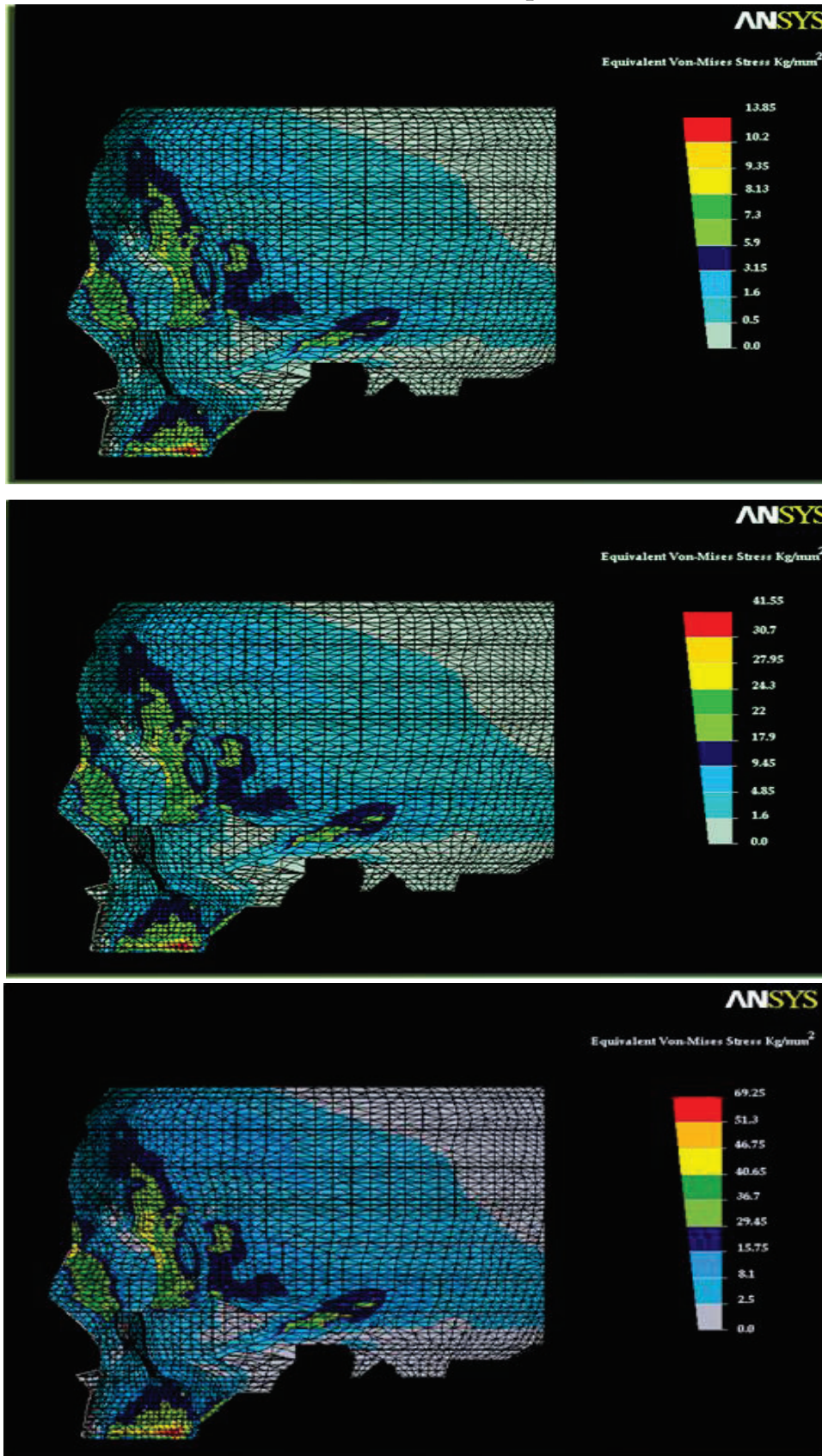


motion perpendicular to this plane. In addition, a zero-displacement and zero-rotation boundary condition was imposed on the nodes along the superior and posterior surface of the skull and along the foramen magnum.

Even though application of a known force is possible with FE modeling, known transversal (X) displacement with magnitudes of 1 mm, 3 mm and 5 mm were applied on the maxillary canine and first permanent molar crown. It was assumed that the two plates of transversal orthopedic appliance moved apart by a total of 2 mm, 6 mm and 10 mm respectively.

The displacements and Von-Mises stresses

Figure 5: Contour plots for stress distribution in craniofacial complex with (A) 1 mm, (B) 3 mm and (C) 5 mm of expansion



in different planes were studied on different nodes located at various structures of the craniofacial complex. The stress distribution patterns were analyzed; the results were tabulated and graphically represented.

Results

The biomechanical changes observed in this study were evaluated under the headings:

Table I: Material Properties

Material	Young's Modulus (kg/mm ²)	Poisson's ratio
Tooth	2.07 x 10 ³	0.3
Compact bone	1.37 x 10 ³	0.3
Cancellous bone	7.90 x 10 ²	0.3

Table II: Comparison of the computational result of transversal (X) displacement of the various structures of the craniofacial complex with varying amounts of expansion

Region	Selected nodes on	X (mm)		
		1 mm	3 mm	5 mm
Dentoalveolar	Incisal edge of 1	0.95	2.8	4.45
	Cusp tip of 3	0.82	2.4	4.28
	Cusp tip of 6	0.91	2.6	4.27
	Apical region of 1	0.71	1.41	3.78
	Apical region of 3	0.62	1.21	3.52
	Apical region of 6	0.69	1.51	3.67
Maxilla	Pt. "A "	0.2	1.4	3.9
	ANS	0.14	1.21	3.41
	Tuberosity	0.07	1.01	2.89
	Zyg. buttress	0.07	0.8	1.92
	Inf. orb. rim	0	0.31	0.82
	Frontal process	0	0.21	0.57
Palate	Anterior	0.27	1.34	3.54
	Posterior	0.02	0.94	1.84
Nasal cavity wall	Anteroinferior	0.51	1.06	3.24
	Anterosuperior	0.02	0.76	1.08
	Posteroinferior	0.01	0.8	1.7
	Posterosuperior	0	0.16	0.35
Nasal bone	Superior	0	0	0
	Inferior	0	0.03	0.15
Sphenoid bone	Medial pterygoid inferior	0	0.97	2.04
	Medial pterygoid superior	0	0.5	1.18
	Lateral pterygoid inferior	0	1.1	2.34
	Lateral pterygoid superior	0	0.11	0.32
	Greater wing	0	0.06	0.21
Zygomatic bone	Frontal process	0	0.23	1.62
	Zyg. arcus anterior	0	0.03	0.21
	Zyg. arcus posterior	0	0	0
	Body	0	0	0.07
Frontal bone	Supraorbital	0	0	0
	Forehead	0	0	0
Temporal	Squamous	0	0.02	0.15

Table III: Comparison of the computational result of sagittal (Y) displacement of the various structures of the craniofacial complex with varying amounts of expansion

Region	Selected nodes on	Y(mm)		
		1 mm	3 mm	5 mm
Dentoalveolar	Incisal edge of 1	0	0.11	0.35
	Cusp tip of 3	0	0.03	0.15
	Cusp tip of 6	0	0.24	0.74
	Apical region of 1	0	0.34	0.78
	Apical region of 3	0	0.21	0.5
	Apical region of 6	0	0.11	0.34
Maxilla	Pt. "A "	0	0.18	0.54
	ANS	0	0.21	0.72
	Tuberosity	0	0.02	0.12
	Zyg. buttress	0	0	0
	Inf. orb. rim	0	0	0.02
	Frontal process	0	0	0.02
Palate	Anterior	0.17	0.74	1.21
	Posterior	0.09	0.68	1.09
Nasal cavity wall	Anteroinferior	0	0.09	0.24
	Anterosuperior	0	0	0.12
	Posteroinferior	0.07	0.15	0.21
	Posterosuperior	0	0	0
Nasal bone	Superior	0	0	0
	Inferior	0	0	-0.12
Sphenoid bone	Medial pterygoid inferior	0	-0.2	-0.6
	Medial pterygoid superior	0	-0.07	-0.12
	Lateral pterygoid inferior	0	0.1	0.26
	Lateral pterygoid superior	0	0	0.1
	Greater wing	0	-0.06	-0.21
Zygomatic bone	Frontal process	0	-0.27	-0.71
	Zyg. arcus anterior	0	-0.34	-0.82
	Zyg. arcus posterior	0	-0.09	-0.32
	Body	0	-0.18	-0.27
Frontal bone	Supraorbital	0	0	0
	Forehead	0	0	0
Temporal	Squamous	0	0	0

- 1) Displacement of different bones of the craniofacial complex with varying amounts of transverse expansion.
- 2) Stress distribution observed at different bones of the craniofacial complex with varying amounts of transverse expansion.

Displacements of the craniofacial structures were studied in 3 dimensions: transversal – (X) plane, sagittal –(Y) plane and vertical –(Z) plane. Positive value (+) indicated an anterior movement in a sagittal (Y) plane and an upward movement in the vertical (Z) plane.

Negative value (-) indicated a posterior movement in a sagittal (Y) plane and a downward movement in the vertical (Z) plane.

Displacement in the transverse plane: (X-displacement) (Table II)

Maximum X-displacement (lateral displacement) was 4.45 mm at node corresponding to the incisal edge of upper central incisor. Displacements were noted more in the dentoalveolar region compared to the skeletal changes.

Table IV: Comparison of the computational result of transversal (X), sagittal (Y), and vertical (Z) displacement of the various structures of the craniofacial complex with varying amounts of expansion

Region	Selected nodes on	Z(mm)		
		1 mm	3 mm	5 mm
Dentoalveolar	Incisal edge of 1	-0.12	-0.3	-0.65
	Cusp tip of 3	0	0.12	0.32
	Cusp tip of 6	0	0.08	0.26
	Apical region of 1	0	-0.2	-0.5
	Apical region of 3	0	0.09	0.21
	Apical region of 6	-0.02	-0.08	-0.14
Maxilla	Pt. "A "	-0.01	-0.45	-1.02
	ANS	0	-0.34	-0.98
	Tuberosity	0	0.09	0.17
	Zyg. buttress	0.07	0.17	0.36
	Inf. orb. rim	0	0.09	0.22
	Frontal process	0	0	0.07
Palate	Anterior	0	-0.3	-0.87
	Posterior	0	-0.24	-0.92
Nasal cavity wall	Anteroinferior	0	0	-0.24
	Anterosuperior	0	0	-0.03
	Posteroinferior	0	0	-0.14
	Posterosuperior	0	0	-0.03
Nasal bone	Superior	0	0	0
	Inferior	0	-0.09	-0.37
Sphenoid bone	Medial pterygoid inferior	0	-0.31	-0.82
	Medial pterygoid superior	0	0	0.9
	Lateral pterygoid inferior	0	-0.31	-0.87
	Lateral pterygoid superior	0	0.14	0.1
	Greater wing	0	0.08	0.24
Zygomatic bone	Frontal process	0	0.34	0.98
	Zyg. arcus anterior	0	0.11	0.34
	Zyg. arcus posterior	0	0	0.02
	Body	0.12	0.28	0.7
Frontal bone	Supraorbital	0	0	0
	Forehead	0	0	0
Temporal	Squamous	0	0	0

With 1 mm of separation of expansion device on each side, changes were evident only in the dentoalveolar region and anterior maxillary region. As the expansion device was further separated, displacements of the adjacent structures were noticeable.

Expansion was more in anterior maxillary area compared to the posterior. From the frontal view, pyramidal displacement of maxilla away from the midline was evident.

The width of the nasal cavity at the floor of the nose increased markedly where as the

posterosuperior part of the nasal cavity had moved minimally in the lateral direction. No significant lateral displacement was observed at the temporal, frontal and sphenoid bone. The inferior parts of the pterygoid plates, however, demonstrated lateral displacement or bending. But minimum displacement was observed in the region close to the cranial base, where the plates were more rigid.

Displacement in the anteroposterior plane: (Y - displacement) (Table III)

Table V: Comparison of maximum Von-Mises stresses on the various structures of the craniofacial complex with varying amounts of transverse expansion

Region	Selected nodes on	Max. Von-Mises stress (Kg/mm ²)		
		1 mm	3 mm	5 mm
Dentoalveolar	Incisal edge of 1	0.22	0.45	0.81
	Cusp tip of 3	0.9	2.1	2.7
	Cusp tip of 6	1.4	2	3.4
	Apical region of 1	0.94	1.72	3.21
	Apical region of 3	12.41	18.06	22.32
	Apical region of 6	12.57	16.07	20.71
Maxilla	Pt. "A"	0.8	1.8	2.6
	ANS	0.8	1.64	2.14
	Tuberosity	0.92	1.72	3.24
	Zyg. buttress	2.5	4.72	6.04
	Inf. orb. rim	0.62	1.24	2.02
	Frontal process	0.57	1.12	2.12
Palate	Anterior	0.49	0.92	1.21
	Posterior	0.8	1.27	3.24
Nasal cavity wall	Anteroinferior	5.24	13.84	20.42
	Anterosuperior	1.02	3.41	4.98
	Posteroinferior	1.82	4.27	6.28
	Posterosuperior	0.71	1.37	2.02
Nasal bone	Superior	2.4	7.34	12.14
	Inferior	4.1	10.21	15.28
Sphenoid bone	Medial pterygoid inferior	2.1	8.94	14.24
	Medial pterygoid superior	7.24	57.24	74.24
	Lateral pterygoid inferior	1.84	7.53	12.24
	Lateral pterygoid superior	8.24	55.14	68.17
	Greater wing	3.24	34.27	51.24
Zygomatic bone	Frontal process	3.17	14.04	22.04
	Zyg. arcus anterior	1.61	3.54	7.24
	Zyg. arcus posterior	0.8	1.84	2.14
	Body	1.41	3.71	5.24
Frontal bone	Supraorbital	0.9	1.37	2.8
	Forehead	0.27	0.83	1.02
Temporal	Squamous	0	0.01	0.02

Maximum positive Y-displacement (forward displacement) was 1.21 mm at node representing the anterior aspect of palate followed by 1.09 mm at posterior aspect. All the dentoalveolar structures, maxillary structures, and structures on nasal cavity wall demonstrated forward displacement to varying extent. These changes were evident when the expansion was beyond 3 mm on each side.

Maximum negative Y-displacement (backward displacement) of 0.82 mm was

noted at the node representing the anterior region of zygomatic arc. Overall, the zygomatic bone displayed a backward displacement.

Displacement in the vertical plane: (Z - displacement) (Table IV)

Maximum positive Z-displacement (upward displacement) was 0.98 mm at node representing the frontal process of the zygomatic bone. Maximum negative Z-displacement (downward displacement) was

Region	Selected nodes on	X (mm)			Y (mm)			Z (mm)		
		Iseri et al	Jafari et al	Present study	Iseri et al	Jafari et al	Present study	Iseri et al	Jafari et al	Present study
Dentoalveolar	Incisal edge of 1	5	5.31	4.45	1.4	0.85	0.35	-1.4	-0.45	-0.65
	Cusp tip of 6	5	5.31	4.27	1.4	0.74	0.15	-0.8	0.26	0.26
	Apical region of 1	4.99	4.34	3.78	2.1	0.85	0.74	-1.2	-0.59	-0.5
	Apical region of 3	4.99	3.94	3.52	2.1	0.5	0.5	-1.1	0.26	0.21
	Apical region of 6	4.91	4.08	3.67	2	0.49	0.34	-0.4	0.29	-0.14
Maxilla	Anterior part of palate	4.9	3.22	3.54	2.1	1.03	1.21	-1.1	-0.61	-0.87
	Posterior part of palate	4.8	2.06	1.84	2.1	1.05	1.09	-0.2	-1.02	-0.92
Sphenoid bone	Lateral pterygoid inferior	4.9	2.07	2.34	1.8	0.59	0.26	-0.04	-0.44	-0.87
	Lateral pterygoid superior	1.4	0.44	0.32	1.6	0.08	0.1	-0.7	0.13	0.1
Zygomatic bone	Frontal process	3.9	2.07	1.62	1.6	-0.98	-0.71	-0.4	1.42	0.98
	Zyg. arcus anterior	3.3	0.44	0.21	0.7	-0.93	-0.82	0.4	1.67	0.34
	Zyg. arcus posterior	0.6	0.04	0	-0.04	-0.38	-0.32	0.2	0.06	0.02
Nasal cavity wall	Anteroinferior	4.8	3.25	3.24	2.1	0.52	0.24	-1.1	0	-0.24
	Anterosuperior	4.8	1.26	1.08	2.1	0.16	0.12	-0.02	-0.02	-0.03
	Posterosuperior	-0.3	0.65	0.35	0.2	0.02	0	-1.1	-0.02	-0.03
Nasal bone	Body	0.3	0.23	0.15	-1.2	-0.5	-0.12	-1.1	-0.59	-0.37
Frontal bone	Supraorbital	0.03	0.01	0	-0.2	-0.02	0	-0.5	0.1	0
Temporal	Squamous	0.1	0.6	0.15	0.08	-0.25	0	0.4	0.59	0

1.02 mm of point 'A', indicating a downward displacement of maxilla. Considering both these points, it is evident that the nasomaxillary complex rotated in such a manner that the lateral structures had moved upward and midline structures downward. The anterior part of the maxillary bone (point A and ANS) and maxillary central incisors were displaced downward.

Comparison of maximum Von-Mises stresses on various structures of the craniofacial complex with varying amounts of expansion

Table V shows the comparison of maximum Von-Mises stresses on the various craniofacial structures with varying amounts of expansion. The findings show that the stresses at the nodes varied linearly for the given displacement boundary conditions due to RME.

Initial stress images of the three-dimensional model of skull are as shown in Fig 5 A, B and C. The areas of stress are shown with the help of different colours. The pellets of colours representing the tensile and compressive

stresses are shown on the right-hand side of the diagram. Using the computer-generated colour diagrams the following results were obtained.

In the dentoalveolar region, the stresses were high in apical region of canine and first molar and they continued to increase as the expansion progressed. In the maxilla, zygomatic buttress demonstrated high stress values compared to the other areas evaluated. The posterior region of the palate demonstrated higher stress values compared to the anterior region. The anteroinferior region of the nasal cavity demonstrated stresses in range of 5.24 - 20.42 kg/mm², which were highest for the areas assessed.

Highest stress levels were observed in the pterygoid plates of sphenoid bone. The findings indicated that high stresses produced by RME are especially located in the superior parts of the pterygoid processes of the sphenoid bone (74.24 kg/mm² at medial and 68.17 kg/mm² at lateral pterygoid). The greater wing of sphenoid also demonstrated high stress levels (51.24 kg/mm²).

Discussion

Finite element analysis is a mathematical method in which the shape of complex geometric objects and their physical properties are computer constructed. Interactions of various components of the model are then calculated for stress, strain and deformation. This method was first used in orthodontics by Thresher and Saito (1973)[8] to study stresses in human teeth. Ever since, this method has proved effective in many dental fields such as simulation of tooth movement and optimization of orthodontic mechanics. Such an extensive use has been primarily done because of its advantages. The method is non-invasive; the actual amount of stress experienced at any given point can be theoretically measured; the tooth, alveolar bone, periodontal ligament, and craniofacial bones can be simulated; the displacement of the tooth and the craniofacial complex can be visualized graphically; the point of application, magnitude, and direction of a force may easily be varied to simulate the clinical situation, reproducibility does not affect the physical properties of the involved material; and the study can be repeated as many times as the operator wishes.

The 3-dimensional FEM used in the present study provided the freedom to simulate orthodontic force systems applied clinically and allowed analysis of response of the craniofacial skeleton to the orthodontic loads in three-dimensional space.

The experimental method employed in this study permitted the visualization of bone reactions, even with the lowest loading degree. One should be aware that the structural and spatial relationships of various craniofacial components vary among individuals. It is important to realize that these factors may contribute to the varied responses of the craniofacial components on loading *in vivo*. Thus, the results of this study are valid only for a single specific human skull.

This can be seen as a problem in generalizing the findings obtained in this study. On the

other hand, studies done by Iseri *et al*[7] and Jafari *et al*[6] yielded same results in spite of the differences in method used and the variation in skull geometry. Iseri *et al*[7] used CT images of a 12-year old patient while Jafari *et al*[6] constructed the model from CT images of dry human skull with an approximate age of 12 years. They showed that, although there were differences in the craniofacial structures between subjects, the responses to the same mechanical forces were same in the FEM.

So, though there were quantitative differences (Table VI), qualitatively, the mechanical response was predicted in the same manner, which is a positive indication for the validity of the qualitative conclusions.

Though we used an adult human skull to develop the finite element model, the displacements of the various craniofacial structures were compared with similar corresponding structures of the previous studies.[6,7]

Overall pattern of displacement

The pattern of displacement revealed that the greatest widening was observed in the dento-alveolar structures, with the expansion effect gradually decreasing towards the superior structures. The results of the present study support those of the previous studies[6,7], which reported the maxillary suture to separate supero-inferiorly in a non-parallel manner, the separation being pyramidal in shape with base of the pyramid located at the oral side of the bone and the centre of rotation located near the frontonasal suture.

In the sagittal (Y) plane, the structures along the midline showed an anterior displacement while the lateral structures demonstrated a posterior displacement.

In the vertical (Z) plane, the entire maxillary complex descended downwards more or less in a parallel manner while the lateral structures demonstrated an upward displacement.

Overall pattern of stress distribution

Stresses produced by the expansion appliance were concentrated in the anterior region of the palate. The initial effects of the expansion were observed at region of central incisors.

With increased activations, stresses radiated from the midpalatine area superiorly along the perpendicular plates of the palatine bone to deeper anatomic structures. The buttressing of the maxillary tuberosity with the pterygoid plates of the sphenoid bone allowed the forces to then radiate to the base of the medial pterygoid plate.

From this region, the stresses then spread further superiorly toward the malar and the zygomatic bones.

Heavy stresses were observed in the area of the base of pterygoid plates of sphenoid bone. *These areas of stress concentration indicate regions of potential weakness or regions where major biologic responses may be expected.*

If the maxilla is fused to the pterygoid plates, as is the probable case in adult patients, intermaxillary expansion would be difficult to obtain, regardless of how much the suture between the two halves of maxilla are affected by the orthopedic forces.

Unlike the maxillae, the pterygoid processes are not individual bones, but parts of the same cranial bone - the sphenoid. So, even if surgically assisted rapid maxillary expansion (SA-RME) is advocated, the osteotomized maxillae and palatine bones would move apart on application of expansion forces, but the fused pterygoid processes which cannot separate, tend to splay outward.

In children and adolescents, the midpalatal and circummaxillary sutures generate less resistance to expansion forces, thus limiting the development of internal stresses in the dentoalveolar region. Consequently, maxillary expansion is accompanied by sutural adjustments in the craniofacial complex in remote regions, rather than by alveolar remodeling or tipping. However, these adaptive changes cannot be exploited following skeletal maturation because the

sutures are no longer patent and the expansion forces are now resisted by the reinforcing buttresses of the midfacial skeleton. The heavy stresses at the pterygoid plates can radiate across to deeper anatomic structures, including the body and greater wings of sphenoid bone thereby denoting far-reaching effects of orthopedic expansion of maxilla in adults.

Contrary to conventional perception, this study along with the previous studies^{6,7,9,10} disclosed that resistance provided by the pterygomaxillary articulations was greater than that of the zygomaticomaxillary buttresses.

The results of the present study using the three-dimensional FEM of an Adult Human Skull provided explanation about the mechanical reactions of the bony tissues, which are the first steps in the complex and dynamic process of tissue response to maxillary expansion.

However, as stated previously, FE method has certain limitations, most important being the results applicable only to the FE model created. It may not necessarily apply to all individuals quantitatively. However, what is important is that most of them, would give **QUALITATIVELY THE SAME RESULTS** as were obtained in the present study, which can prove useful if employed judiciously.

The present study is precisely for the purpose of highlighting the qualitative differences in biomechanical effects of RME employed in an adult. Simulation models that are being used for diagnostic, operational planning or rehearsal purposes in the field of medical sciences can be effectively and efficiently employed in the field of orthodontics and maxillofacial surgery.

Conclusion

It can be thus concluded from the present study that:

- Finite element analysis is a valid, reliable and fairly accurate method of analysis of

stresses generated in the craniofacial complex.

- Accurate geometric model of craniofacial skeleton should be created to study the displacement and stresses in the craniofacial complex and skeleton.
- Though expansion can be achieved in adults, displacements are noted more in the structures located anteriorly and along the midline while the posterior and lateral structures demonstrate minimal displacement but high stresses.
- Rapid maxillary expansion must be used judiciously in adults, because of its far-reaching effects involving heavy stresses being noted at the sphenoid bone, zygomatic bone, nasal bone and their adjacent sutures.
- Specific responses in individual cases, especially in adults, can be predetermined with the use of simulation models and the design of treatment mechanics, accordingly tailored.

It is hoped that this further exploration of the skeletal and dental effects of transverse orthopedic forces better defines the parameters of clinical expectations from this orthopedic procedure when employed in adults.

References

1. Cameron CG, Franchi L, Baccetti T, McNamara JA. Long-term effects of rapid maxillary expansion. A posteroanterior cephalometric evaluation. *Am J Orthod Dentofac Orthop.* 2002; 121: 129-35.
2. Bishara SE, Staley RN. Maxillary expansion: clinical implications. *Am J Orthod Dentofac Orthop.* 1987; 91: 3-14.
3. Proffit WR, Fields HW, Ackerman JL, Bailey LT, Tulloch JFC. Contemporary Orthodontics. 3rd Ed. St. Louis: Mosby Inc; 2000.
4. McNamara JA Jr, Brudon WL. Orthodontic and orthopedic treatment in the mixed dentition. Ann Arbor, Mich: Needham Press; 1993.
5. Tanne K, Harage J, Kakiuchi K, Uamagat Y, Sakuda M. Biomechanical effect of anteriorly directed extraoral forces on the craniofacial complex: A study using the finite element method. *Am J Orthod Dentofac Orthop.* 1989; 95: 200-7.
6. Jafari A, Shetty KS, Kumar M. Study of stress distribution and displacement of various craniofacial structures following application of transverse orthopedic forces. A three-dimensional FEM study. *Angle Orthod.* 2003; 73: 12-20.
7. Iseri H, Tekkaya AE, Oztano, Bilgic S. Biomechanical effects of rapid maxillary expansion on the craniofacial skeleton, studied by the finite element method. *Eur J Orthod.* 1998; 20: 347-56.
8. Thresher RW, Saito GE. The stress analysis of human teeth. *J Biomech.* 1973; 6: 443-9. Cited in Tanne K, Sakuda M, Burstone CJ. Three-dimensional finite element analysis for stress in the periodontal tissue by orthodontic forces. *Am J Orthod Dentofac Orthop.* 1987; 92: 499-505.
9. Chaconas SJ, Caputo AA. Observation of orthopedic force distribution produced by maxillary orthodontic appliances. *Am J Orthod.* 1982; 82: 492-501.
10. Shetty V, Mendoca Caridad J, Caputo AA, Chaconas SJ. Biomechanical rationale for surgical-orthodontic expansion of the adult maxilla. *J Oral Maxillofac Surg.* 1994; 52: 742-749.